J. Synchrotron Rad. (1998). **5**, 929–931

New high- and low-temperature apparatus for synchrotron polycrystalline X-ray diffraction

C. C. Tang, G. Bushnell-Wye and R. J. Cernik*

CCLRC Daresbury Laboratory, Warrington, Cheshire WA4 4AD, UK. E-mail: r.j.cernik@dl.ac.uk

(*Received 4 August 1997; accepted 4 December 1997*)

A high-temperature furnace with an induction heater coil and a cryogenic system based on closed-cycle refrigeration have been assembled to enhance the non-ambient powder diffraction facilities at the Synchrotron Radiation Source, Daresbury Laboratory. The commissioning of the high- and low-temperature devices on the high-resolution powder diffractometer of Station 2.3 is described. The combined temperature range provided by the furnace/cryostat is 10–1500 K. Results from Fe and NH_4Br powder samples are presented to demonstrate the operation of the apparatus. The developments presented in this paper are applicable to a wide range of other experiments and diffraction geometries.

Keywords: induction furnaces; closed-cycle cryostats; synchrotron X-ray powder diffraction.

1. Introduction

Many interesting physical phenomena exhibited by materials have been discovered at non-ambient temperatures. It is therefore not surprising to have seen the construction of high- and low-temperature devices for powder diffraction for many years. The different kinds of furnace and cryostat, and their design features, have been reviewed in detail by McKinstry (1970), Aldebert (1984) and Rudman (1976). At Daresbury Laboratory, high-resolution powder diffraction (HRPD) studies are routinely carried out at room temperature on Stations 2.3 and 9.1. Facilities also exist for high-temperature (resistive heating) and low-temperature (He-flow cryostats) studies, but their reliability and operating range in a multi-user context have proved to be inadequate. As we are dedicated to enhancing our diffraction facilities, we have developed apparatus for non-ambient temperature measurements. Combined with the inherently high-resolution instrument, and the improved cryogenic and furnace technologies, we have recently commissioned an induction furnace and a closed-cycle cryostat for X-ray diffraction (XRD) studies. These are of particular interest in the investigation of lattice thermal expansion and of structural phase transitions. In this paper, we describe the commissioning of the induction furnace and the cryostat carried out at Station 2.3. XRD measurements for Fe and NH_4Br powder samples are presented.

2. Station 2.3 – HRPD

The diffraction instrument of Station 2.3 was initially constructed for ambient HRPD studies (Cernik *et al.*, 1990; Collins *et al.*, 1992) based on the parallel beam optics of Parrish *et al.* (1986). Briefly, the station is situated about 15 m tangentially from a 1.2 T dipole magnet in the 2 GeV electron storage ring receiving X-rays in the range 0.7–2.5 Å. The polychromatic beam from the synchrotron is filtered by a water-cooled Si(111) channel-cut single crystal. A monochromatic X-ray beam of 2×8 mm, incident at the centre of the two-circle (θ and 2θ) diffractometer, is monitored by a scintillation counter. The diffracted beam passes through the parallel foil assembly on the 2θ arm and finally reaches the detector, which is an enhanced dynamic range scintillation counter (0.5–10^6 counts s^{-1}). The parallel foils have a nominal angular acceptance angle of 0.06° with an overall aperture of 20×20 mm. The furnace or the cryostat can be mounted on the θ-circle with a flat-plate sample holder inside the device so that the Hart & Parrish (1986) diffraction geometry is achieved. In such geometry, the diffraction optics are insensitive to changes in the sample height. This is essential as small movements are inevitable when the sample is subjected to cooling or heating.

3. Induction furnace

The induction furnace, powered by a 1 kW supply unit, is an in-house development. The construction is based on the design features described by Debrenne *et al.* (1970). The furnace body of 20 cm diameter and 15 cm depth is made from stainless steel and weighs about 25 kg. To prevent chemical reaction of the sample with air, the device is evacuated down to 10^{-3} mbar using a Drytel vacuum system. The apparatus and the diffraction geometry are shown schematically in Fig. 1. With the furnace mounted on the θ-circle, the height of the flat-plate holder assembly can be adjusted so that the sample surface is placed at the centre of rotation of the diffractometer. Sample crucibles are made out of carbon or tungsten because of their high melting

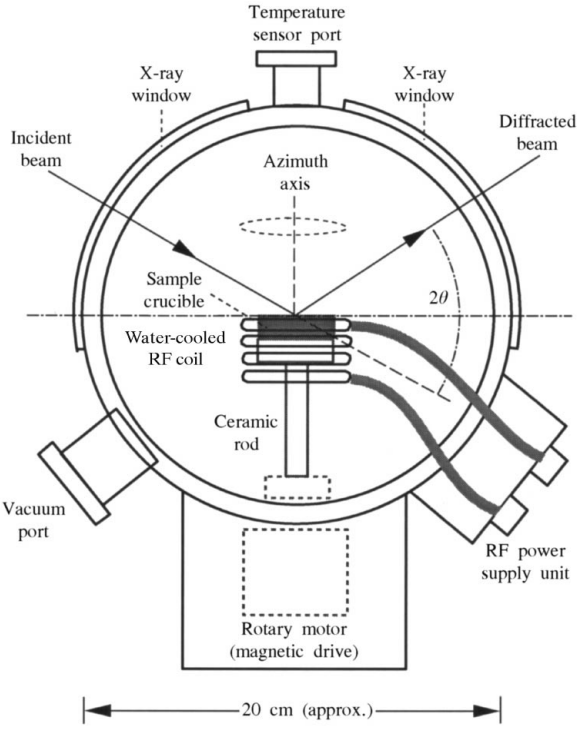

Figure 1
Schematic representation of the induction furnace and the diffraction geometry.

point and induction characteristics. The crucible is supported by a ceramic shaft which is magnetically coupled to an external motor providing sample rotation (~1 revolution s^{-1}) about the azimuth axis. Incident and diffracted X-ray beams pass through the entrance and exit kapton (50 μm thick) windows (Fig. 1). The heating is powered by a water-cooled RF copper coil and is controlled by a Eurotherm 900 unit. Remote temperature control is carried out using a personal computer linked to the control unit. The temperature is measured using a pyrometer (control) and a tungsten–rhenium thermocouple (sample). Note that the thermocouple can be disengaged for spinning-sample measurements. The designed operational temperature range is 290–2000 K but the present power supply unit has a high-temperature limit of 1500 K. However, the heating response time to a set temperature is very fast; about 30 s at 800 K. Even at the higher temperature range, thermal stability of ±1 K can be achieved in less than a few minutes.

4. Cryogenic apparatus

Fig. 2 is a schematic diagram of the assembled cryogenic head and the diffraction geometry. With aluminium thermal and vacuum shields surrounding the sample, an initial vacuum of 10^{-3} mbar has been achieved. Aluminized Mylar windows on the shields allow the entrance and exit of X-ray beams. Including the mounting bracket, it weights about 10 kg with a base diameter of 15 cm and height of 30 cm. The flat-plate sample holder sits on an extended copper block fitted to the cold head (CTI Cryogenics). Pressurized helium is pumped from a compressor to remove heat in the head. The sample holder spindle is connected to a long insulation shaft which is driven externally by a motor to provide sample rotation (~1 revolution per 2 s) about the azimuth axis. Two silicon diode sensors are used for thermal control and for registering the sample temperature. The sensors and the 25 W heater of the cold head are connected through a vacuum port to a Lake Shore temperature controller. Again, remote temperature control is carried out using a personal computer linked to the controller. Note that the sample sensor can be disengaged when measurements are to be taken with a spinning sample. The cryostat has an averaged cooling rate of *ca* 1.6 K min^{-1}. At base temperatures (~10 K) a thermal stability of ±0.5 K has been achieved.

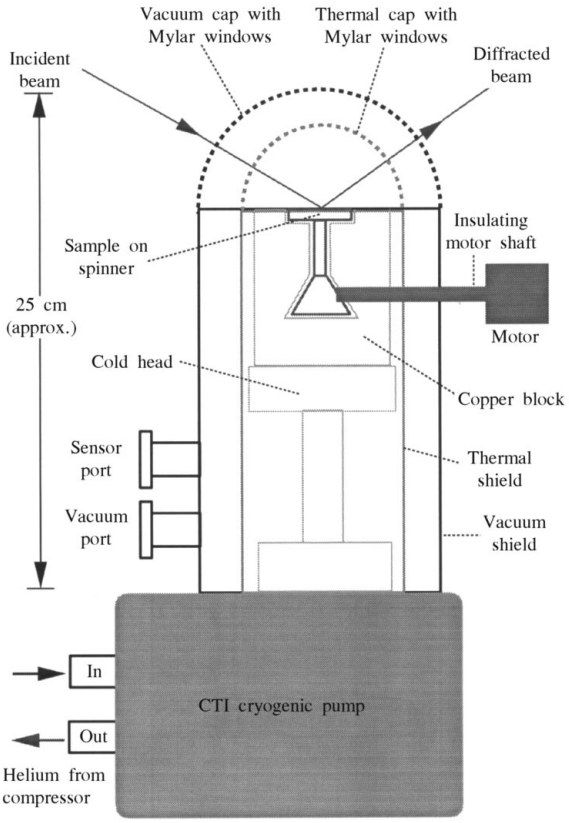

Figure 2
Schematic representation of the cryogenic system and the diffraction geometry.

5. Results

In the high-temperature demonstration, we used fine Fe powder (99.0% purity) to test the apparatus by observing the well known b.c.c. to f.c.c. structural transition of the material ($T \simeq 1180$ K). The low- ($-79 \leq T \leq 1180$ K) and the high-temperature ($1180 \leq$

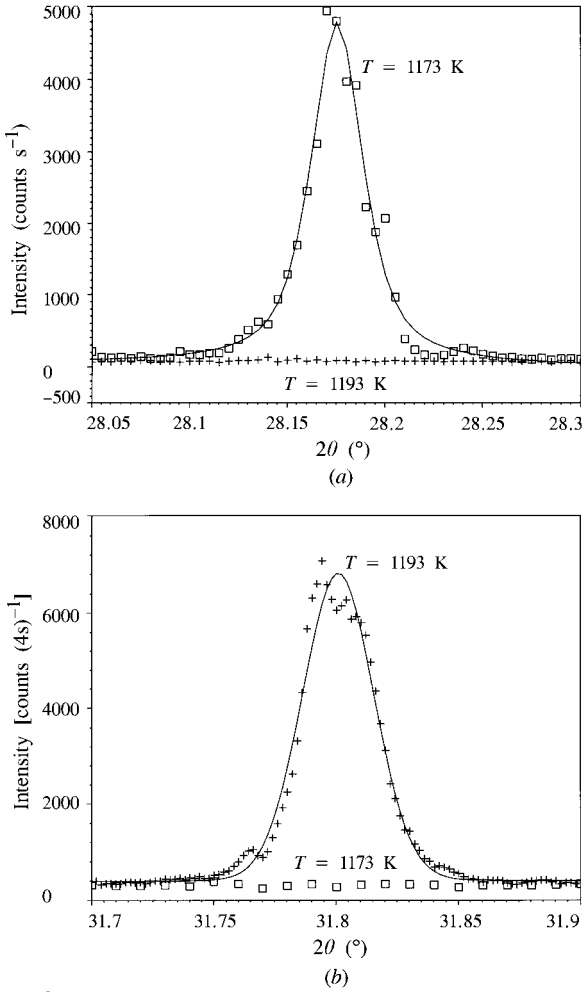

Figure 3
(*a*) The presence and absence of the b.c.c. (110) reflection at $T = 1173$ K (open squares □) and at $T = 1193$ K (crosses +). These measurements were obtained from the Fe powder using an X-ray beam of λ = 1.0 Å. The solid line is the fit of a pseudo-Voigt function to the data (□). (*b*) The absence and presence of the f.c.c. (200) reflection at $T = 1173$ K (open squares □) and $T = 1193$ K (crosses +). The solid line is the fit of a pseudo-Voigt function to the data (+).

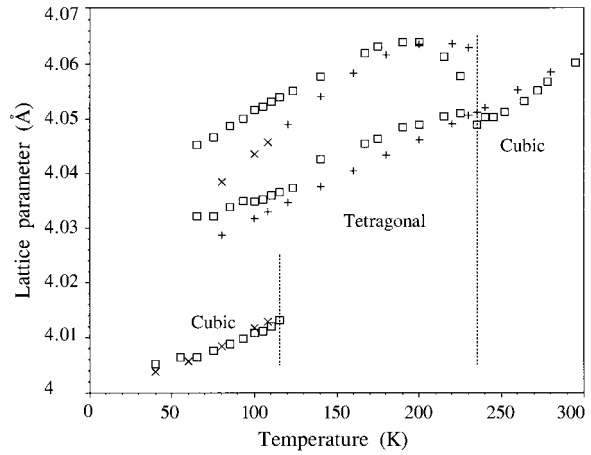

Figure 4
Lattice parameters of NH_4Br as a function of temperature. □ present data; + data of Hovi *et al.* (1965); × data of Bonilla *et al.* (1970).

$T \leq 1660$ K) forms are known as the α- and γ-phases, respectively. When the powder (7 μm maximum particle size) was loaded into the crucible, the furnace temperature was quickly raised to 1173 K, just below the α–γ phase transition. The b.c.c (110) and f.c.c. (200) peak positions were scanned at this temperature using an X-ray beam of $\lambda = 1.0$ Å. The sample was then heated to 1193 K, just above the transition, and the peak positions were scanned again. Fig. 3(*a*) presents the $\theta/2\theta$ scans of the (110) reflection at the two temperatures. The peak has clearly disappeared at the higher temperature, which effectively indicates the collapse of the body-centred structure. In Fig. 3(*b*), however, the emergence of the (200) peak at the higher temperature indicates the development of the face-centred structure in the Fe sample.

Commissioning work on the cryogenic apparatus was carried out in a study of the phase transitions of NH_4Br powder. This material has a simple cubic structure (CsCl) at room temperature ($a_{RT} = 4.0594$ Å), with an NH_4 cation in a cubic framework of bromide ions. At $T \simeq 230$ K, the material undergoes a tetragonal transition, and at $T \simeq 110$ K, the structure transforms back to the CsCl structure (Hovi *et al.*, 1965; Bonilla *et al.*, 1970). Fig. 4 is a summary of our measurements showing the lattice parameter as a function of temperature. The experimental error of less than 0.01% in each measurement is actually smaller than the data point plotted. The general structural behaviour observed in the present study is in agreement with previous results (Hovi *et al.*, 1965; Bonilla *et al.*, 1970). However, there are differences in the rate of lattice expansion. First, the tetragonal expansion rate below 200 K is smaller by comparison while the cubic behaviour at high and low temperatures is very much the same. Secondly, at $T \simeq 90$ K, there is a small but maybe significant anomalous behaviour in the smaller tetragonal cell parameter. A detailed report to explain the structural behaviour is under preparation by Clark *et al.* (1998).

6. Conclusions

Testing and commissioning of the induction furnace was carried out using fine Fe powder. Diffraction measurements were successfully performed at temperatures just below and above the α–γ phase transition. The results have clearly shown the well known structural transition. Using the developed cryogenic system, the lattice parameter of NH_4Br was investigated as a function of temperature. The present study from 40 to 295 K, through the tetragonal and low-temperature cubic phases, revealed interesting and new results. In conclusion, we have successfully commissioned the low- and high-temperature apparatus on the HRPD instrument of Station 2.3, which is now available to the user community.

The authors are grateful to EPSRC (UK) for the provision of beam time. We would also like to thank Dr S. M. Clark and Mr J. C. Guerra Ramon for assistance in the analysis of the NH_4Br data.

References

Aldebert, P. (1984). *Rev. Phys. Appl.* **19**, 649–662.
Bonilla, A., Garland, C. W. & Schumaker, N. E. (1970). *Acta Cryst.* A**26**, 156–158.
Cernik, R. J., Murray, P. K., Pattison, P. & Fitch, A. N. (1990). *J. Appl. Cryst.* **23**, 292–296.
Clark, S. M., Guerra Ramon, J. C. & Tang, C. C. (1998). In preparation.
Collins, S. P., Cernik, R. J., Pattison, P., Bell, A. M. T. & Fitch, A. N. (1992). *Rev. Sci. Instrum.* **63**, 1013–1014.
Debrenne, P., Laugier, J. & Chaudet, M. (1970). *J. Appl. Cryst.* **3**, 493–496.
Hart, M. & Parrish, W. (1986). *Mater. Sci. Forum*, **9**, 39–46.
Hovi, V., Heiskanen, K. & Varteva, M. (1965). *Low Temp. Phys.* **LT9**(B), 1179–1183.
McKinstry, H. A. (1970). *J. Appl. Phys.* **41**, 5074–5079.
Parrish, W., Hart, M., Erickson, C. G., Masciocchi, N. & Huang, T. C. (1986). *Adv. X-ray Anal.* **29**, 243–250.
Rudman, R. (1976). *Low-Temperature X-ray Diffraction: Apparatus and Techniques.* New York: Plenum Press.